

Cite this: *Nanoscale Horiz.*, 2025,  
10, 258

# “Sweet MOFs”: exploring the potential and restraints of integrating carbohydrates with metal–organic frameworks for biomedical applications

Alessio Zuliani,<sup>a</sup> Victor Ramos,<sup>a</sup> Alberto Escudero<sup>ab</sup> and  
Noureddine Khiar<sup>id</sup>\*<sup>a</sup>

The unique features of metal–organic frameworks (MOFs) such as biodegradability, reduced toxicity and high surface area offer the possibility of developing smart nanosystems for biomedical applications through the simultaneous functionalization of their structure with biologically relevant ligands and the loading of biologically active cargos, ranging from small drugs to large biomacromolecules, into their pores. Aiming to develop efficient, naturally inspired biocompatible systems, recent research has combined organic and materials chemistry to design innovative composites that exploit carbohydrate chemistry for the functionalization and structural modification of MOFs. Scientific investigation in the field has seen a significant rise in the past five years, and it is becoming crucial to acknowledge both the limits and benefits of this approach for future investigation. In this review, the latest research results merging carbohydrates and MOFs are discussed, with a particular emphasis on the advances in the field and the remaining challenges, including addressing sustainability and real-case applicability.

Received 15th October 2024,  
Accepted 1st November 2024

DOI: 10.1039/d4nh00525b

rsc.li/nanoscale-horizons

## Introduction

Carbohydrates (CHs), fundamental building blocks of life alongside lipids, proteins, and nucleic acids, have long captivated researchers with their diverse structure and biological functionalities. Beyond their crucial role in biological signaling, CHs exhibit a myriad of other biological functions, including energy storage, organelle protection, modulation of peptide or protein properties, mediating cellular and extracellular interactions, but also immune response, inflammation and tumor cell metastasis.<sup>1</sup> Besides, different CHs mediate interactions with pathogens during the early and crucial stages of infection, as happens with the adherent-invasive and uropathogenic (UPEC) *Escherichia coli*, HIV-1 virus, influenza, Ebola and coronavirus.<sup>2</sup> For example, it has been demonstrated that the entry of SARS-CoV2 pseudo-typed virus into cells can significantly be inhibited by heparin.<sup>3</sup> CHs are also involved in bacterial infection processes. This is the case for *Pseudomonas aeruginosa*, a bacterium that is a leading cause of morbidity and mortality in cystic fibrosis patients and immunocompromised

individuals, which specifically targets galactose and strongly binds to fucose and fucose-containing oligosaccharides to adhere to epithelial cells.

These essential biological interactions, combined with their biocompatibility and biodegradability, make CHs ideal for a wide range of biomedical applications, spanning from glyco-based drugs,<sup>4,5</sup> drug delivery, diagnosis, and imaging to tissue engineering, wound healing, and antiviral/antimicrobial treatments.<sup>6–10</sup> Nevertheless, the direct use of CHs in biomedical applications is often limited by their structural complexity, low affinity, poor stability, rapid degradation in the body, and lack of controlled release of eventually coupled drugs. Additionally, their solubility and targeting abilities can be suboptimal without further modification. As a result, during the last two decades, research has focused on the design of a variety of glyco-nanomaterials capable of addressing these intrinsic limitations of CHs, including hydrogels, nanotubes, liposomes, micelles, nanoparticles, dendrimers, and metal–organic frameworks (MOFs).<sup>11–20</sup> These CH-based nanosystems feature unique characteristics, such as high avidity coupled with specific recognition by various cell surface receptors, which significantly enhance the receptor-mediated uptake of nanocarriers, thanks also to the exploitation of multivalency, *i.e.*, the presence of multiple copies of the same element on the surface of each nanovector.<sup>21</sup> For example, surface modifications employing specific sugars, such as D-mannose, have been demonstrated to increase the receptor-

<sup>a</sup> Asymmetric Synthesis and Nanosystems Group (Art&Fun), Institute for Chemical Research (IIQ), CSIC-University of Seville, 41092 Seville, Spain.  
E-mail: khiaar@iiq.csic.es

<sup>b</sup> Inorganic Chemistry Department, University of Seville, Calle Profesor García González 1, 41012 Seville, Spain





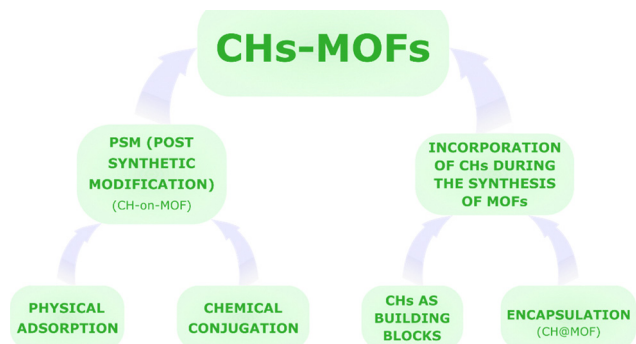


Fig. 1 Scheme of the most common strategies for the preparation of carbohydrate-MOFs (CHs-MOFs).

meaning of the term “saccharide”, from the Latin “*saccharum*”, defined as “. . . a kind of honey found in cane, white as gum, and it crunches between the teeth. . .” (Pliny the Elder), derived from the Ancient Greek word *σάκχαρον* (sakkharon).<sup>48</sup> The review firstly reports a brief discussion of the most studied CHs and MOFs for the preparation of CHs-MOFs. In particular, the biological role and uses of the CHs are summarised as well as the characteristics of the main classes of MOFs studied for biomedical applications. Then, the review is subdivided into two sections, one focused on the most recent strategies for the post synthetic modification (PSM) of MOFs with CHs, forming the so-defined CHs-on-MOFs,<sup>35</sup> and the other focusing on the incorporation of carbohydrates during the synthesis of MOFs, whether as part of the same structure as the MOF or encapsulated in it, *i.e.*, CHs@MOFs,<sup>35</sup> as summarised in Fig. 1. Finally, this review reports some selected examples of preclinical trials of CHs-MOFs, followed by an outlook and conclusion section.

## Most studied carbohydrates and MOFs for the development of CHs-MOFs

### Carbohydrates

Serving as a primary source of energy for living organisms and covering other biological functions ranging from cell signalling and cellular recognition to structural support to cells, CHs, herein referred as a synonym of saccharide,<sup>49</sup> encompass different classes of compounds, *i.e.*, simple monosaccharides, such as glucose and fructose, disaccharides, such as sucrose and lactose, oligosaccharides, containing a small number of sugar units (usually 3–10), and polysaccharides, such as starch, glycogen, and cellulose.

CHs are incorporated into CHs-MOFs to enhance various functional properties, including:

- **Improved biocompatibility:** for example, when CHs are used as building units in CHs-MOFs, their degradation products are non-toxic, minimizing concerns related to toxicity.
- **Enhanced solubility and dispersibility:** the hydrophilic nature of CHs boosts the aqueous solubility and colloidal stability of MOFs, improving their behaviour in biological systems.
- **Enhanced avidity:** to offset the intrinsically low affinity associated with monomeric carbohydrate–protein binding interactions.<sup>50</sup>
- **Targeting capabilities:** specific CHs can be designed to interact with cellular receptors, enabling targeted delivery of drugs or imaging agents to specific tissues or cell types.
- **Controlled release of active compounds:** CHs-MOFs can be engineered to regulate the release kinetics of encapsulated drugs or other active agents, ensuring sustained or stimuli-responsive delivery. For example, CHs can also function as “gatekeepers” by forming a film around drug-loaded MOFs,

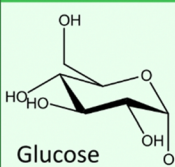
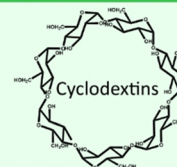
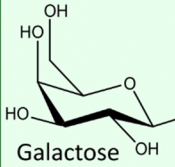
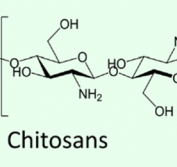
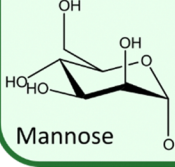
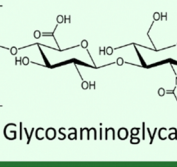
Monosaccharides	Polysaccharides
 <p><b>Glucose</b></p> <ul style="list-style-type: none"> <li>- Treat medical conditions</li> <li>- Mainly used in the food industry</li> <li>- Industrial production by hydrolysis of starch</li> </ul>	 <p><b>Cyclodextrins</b></p> <ul style="list-style-type: none"> <li>- Ability to encapsulate hydrophobic substances</li> <li>- Pharmaceuticals, food industry and environmental applications</li> <li>- Industrial production by degradation of starch</li> </ul>
 <p><b>Galactose</b></p> <ul style="list-style-type: none"> <li>- Affinity to receptors of various diseases, as hepatic cancer</li> <li>- Many industrial applications</li> <li>- Industrial production by hydrolysis of lactose</li> </ul>	 <p><b>Chitosans</b></p> <ul style="list-style-type: none"> <li>- Antimicrobial, antioxidant and wound-healing properties</li> <li>- Pharmaceutical and food industry applications</li> <li>- Industrial production by deacetylation of chitin</li> </ul>
 <p><b>Mannose</b></p> <ul style="list-style-type: none"> <li>- Many medical applications especially against cancer</li> <li>- Diverse industrial applications</li> <li>- Industrial production by extraction from plants</li> </ul>	 <p><b>Glycosaminoglycans</b></p> <ul style="list-style-type: none"> <li>- Widely used in medicine</li> <li>- Pharmaceutical, cosmetic and nutraceutical ingredient</li> <li>- Industrial production by extraction from animals</li> </ul>

Fig. 2 Structures of the most studied carbohydrates for the preparation of CHs-MOFs.





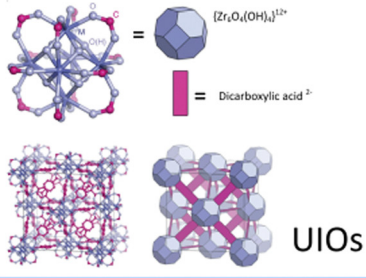
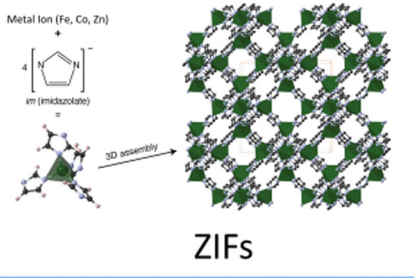
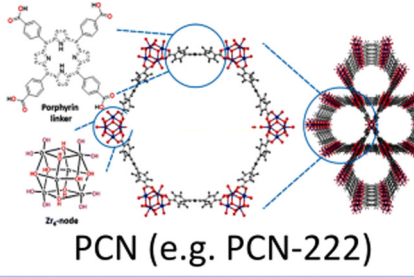
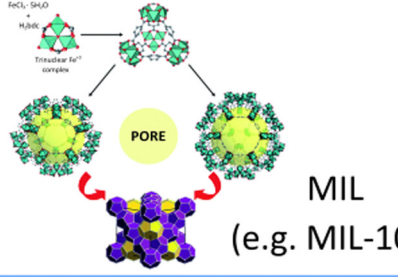
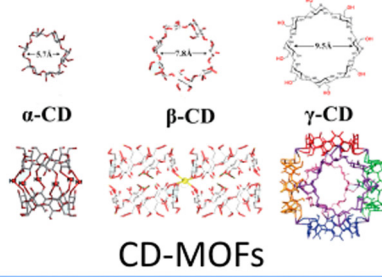
STRUCTURE	PROPERTIES
 <p>UiOs</p>	<ul style="list-style-type: none"> <li>• <math>Zr^{4+}</math> ions + dicarboxylic acid ligands</li> <li>• Pore volumes : <math>0.45 - 1.82 \text{ cm}^3 \text{ g}^{-1}</math></li> <li>• Surface area: <math>1,087 - 4,170 \text{ m}^2 \text{ g}^{-1}</math></li> <li>• Strong bind Zr-O</li> <li>• High porosity, adjustable properties and biocompatibility</li> </ul>
 <p>ZIFs</p>	<ul style="list-style-type: none"> <li>• Tetrahedral transition metal ion + imidazolate</li> <li>• Pore volume: <math>0.34 - 1.24 \text{ cm}^3 \text{ g}^{-1}</math></li> <li>• Surface area: <math>1,200 - 2,000 \text{ m}^2 \text{ g}^{-1}</math></li> <li>• Zeolite-like topologies</li> <li>• Hydrophobic pores and surface</li> <li>• Biocompatibility</li> </ul>
 <p>PCN (e.g. PCN-222)</p>	<ul style="list-style-type: none"> <li>• Metal transition ion + multi-topic organic ligand</li> <li>• Pore volume: <math>0.5 - 2.0 \text{ cm}^3 \text{ g}^{-1}</math></li> <li>• Surface area: <math>1,200 - 4,500 \text{ m}^2 \text{ g}^{-1}</math></li> <li>• High loading capacities and control release</li> <li>• Limited to operate at <math>\text{pH} &lt; 7</math></li> </ul>
 <p>MIL (e.g. MIL-101)</p>	<ul style="list-style-type: none"> <li>• Metal ion/cluster + derived of terephthalic acid</li> <li>• Pore volume: <math>0.34 - 1.37 \text{ cm}^3 \text{ g}^{-1}</math></li> <li>• High surface area: <math>1,500 - 5,900 \text{ m}^2 \text{ g}^{-1}</math></li> <li>• Efficient drug loading (drug delivery)</li> <li>• Biodegradable with biocompatible metal ions</li> <li>• Natural elimination from the body</li> </ul>
 <p>CD-MOFs</p>	<ul style="list-style-type: none"> <li>• Metal ions (K, Ca, Zn) + cyclodextrins</li> <li>• Pore volume: <math>0.45 - 1.80 \text{ cm}^3 \text{ g}^{-1}</math></li> <li>• Surface area <math>1,000 - 3,000 \text{ m}^2 \text{ g}^{-1}</math></li> <li>• Hydrophobic cavities within the cyclodextrin</li> <li>• Effective encapsulating guest molecules</li> <li>• Suitable for biomedical applications</li> </ul>

Fig. 3 Structures and relevant features of the most studied MOFs for the preparation of CHs-MOFs.

some approaches involve the introduction of structural defects with specific organic compounds, such as in the case of the utilization of amino terephthalic acids in UiO-66, or coating MOFs with long-chain molecules like poly ethylene glycols (PEGs) or polysaccharides.

- Shape and size: when discussing the shape and size of nanoparticles for biomedical applications, which are crucial for the circulation in the body and ability to penetrate cells, especially for targeting applications, the literature offers a complex range of perspectives and sometimes conflicting







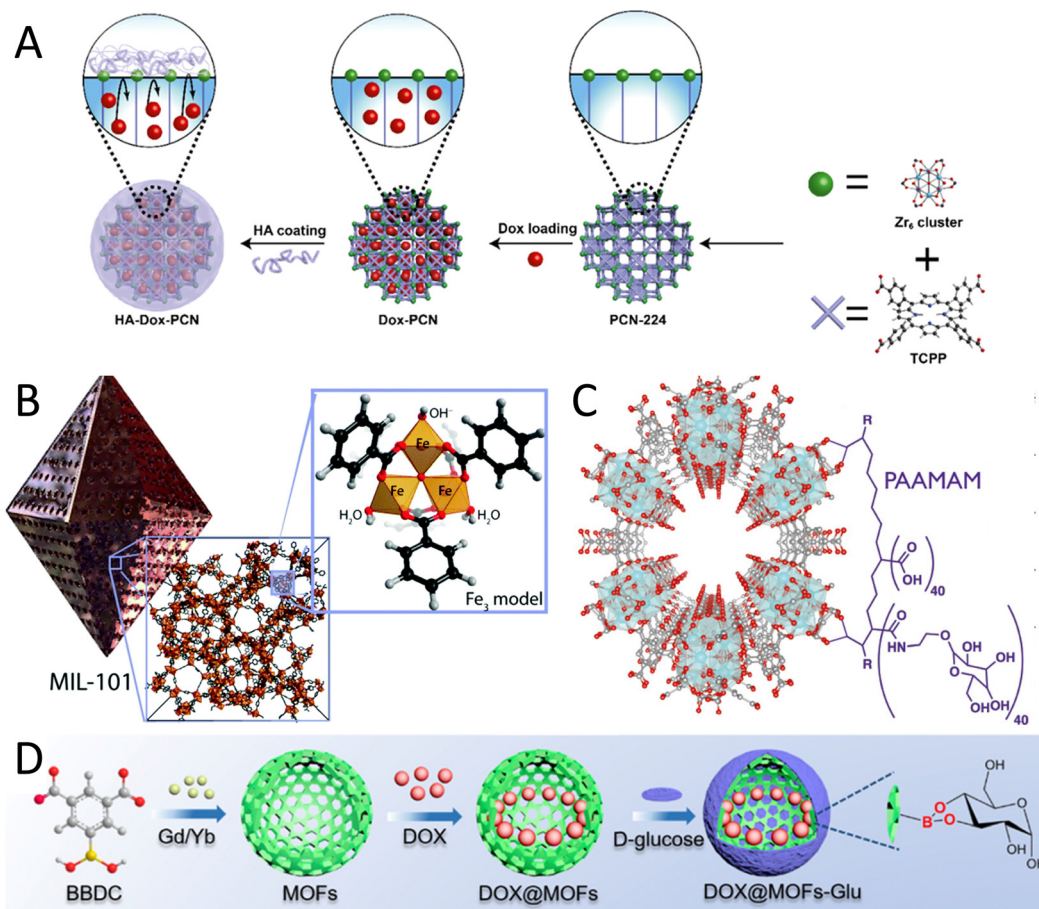


Fig. 4 Examples of CH-on-MOF nanostructures. (A) Coating of the PCN-224 nanoMOF with HA, via their carboxylate groups. Taken from ref. 51 and reproduced with permission from the American Chemical Society, copyright 2019. (B) Heparin is able to complex with the metal sites of the MIL-101(Fe) MOF through its sulfate groups. Taken from ref. 71 and reproduced with permission from the Royal Society of Chemistry, copyright 2018. (C) A poly(acrylic acid-mannose acrylamide) (PAAMAM) glycopolymer containing carboxylate groups is used for the functionalization of the MOF-808. Taken from ref. 27 published by the American Chemical Society, copyright 2022. (D) Synthesis of a MOF-glucose nanocarrier loaded with DOX. Taken from ref. 72 and reproduced with permission from the American Chemical Society, copyright 2018.

Some monosaccharides can also be attached to the surface of MOFs through chemical or electrostatic interactions. The incorporation of these compounds is particularly advantageous for targeting various overexpressed receptors, thereby enhancing the cellular uptake of nanoparticles by facilitating endocytosis and the effective internalization of therapeutic agents. Importantly, most CHs-MOFs made with monosaccharides, especially those designed for targeting applications, primarily utilize commercially available CHs directly linked to the MOFs, or employ short chemicals as linking agents, without further modifications. While this approach has driven valuable research and contributed to the advancement of innovative nanosystems, it also poses a limitation on ground-breaking discoveries. It does not fully leverage the rich chemistry of CHs for more efficient and selective targeting. Indeed, using simple monosaccharides does not guarantee optimal bio-interactions with targets, which often require substantial chemical modifications, such as the introduction of more polar or nonpolar functional groups. Furthermore, the absence of specific spacers between the monosaccharides and the MOFs creates significant

steric hindrance, further reducing selectivity to targeting sites. This is the case, for example, of a MOF consisting of  $Gd^{3+}$  nodes and 5-boronobenzene-1,3-dicarboxylic acid (BBDC) functionalised with glucose (Fig. 4(D)).<sup>72</sup> This nanoplatform was used for imaging-guided precise chemotherapy by interaction with glucose-transported protein (GLUT1) overexpressed in cancer cells.

Similarly,  $Fe_3O_4$  NPs were first coated with the  $NH_2$ -MIL-100 MOF, and this hybrid system was subsequently incubated with D-mannose in phosphate buffered saline. The monosaccharide was eventually absorbed onto the nanostructure surface, very likely driven by an electrostatic interaction, and this nanosystem was used for the targeted therapy of tumour cells exhibiting high levels of mannose receptor (MR) expression.<sup>76</sup> In another work, a novel CaCu-MOF was firstly loaded with doxorubicin and ovalbumin, thus covered and functionalized by galactosamine-linked HA (Fig. 5(C)). The presence of HA guaranteed the biocompatibility and stability of the MOF, while the galactosamine was aimed at the targeting of the asialoglycoprotein receptor (ASGPR) overexpressed on hepatic cancer cells.<sup>77</sup> In all



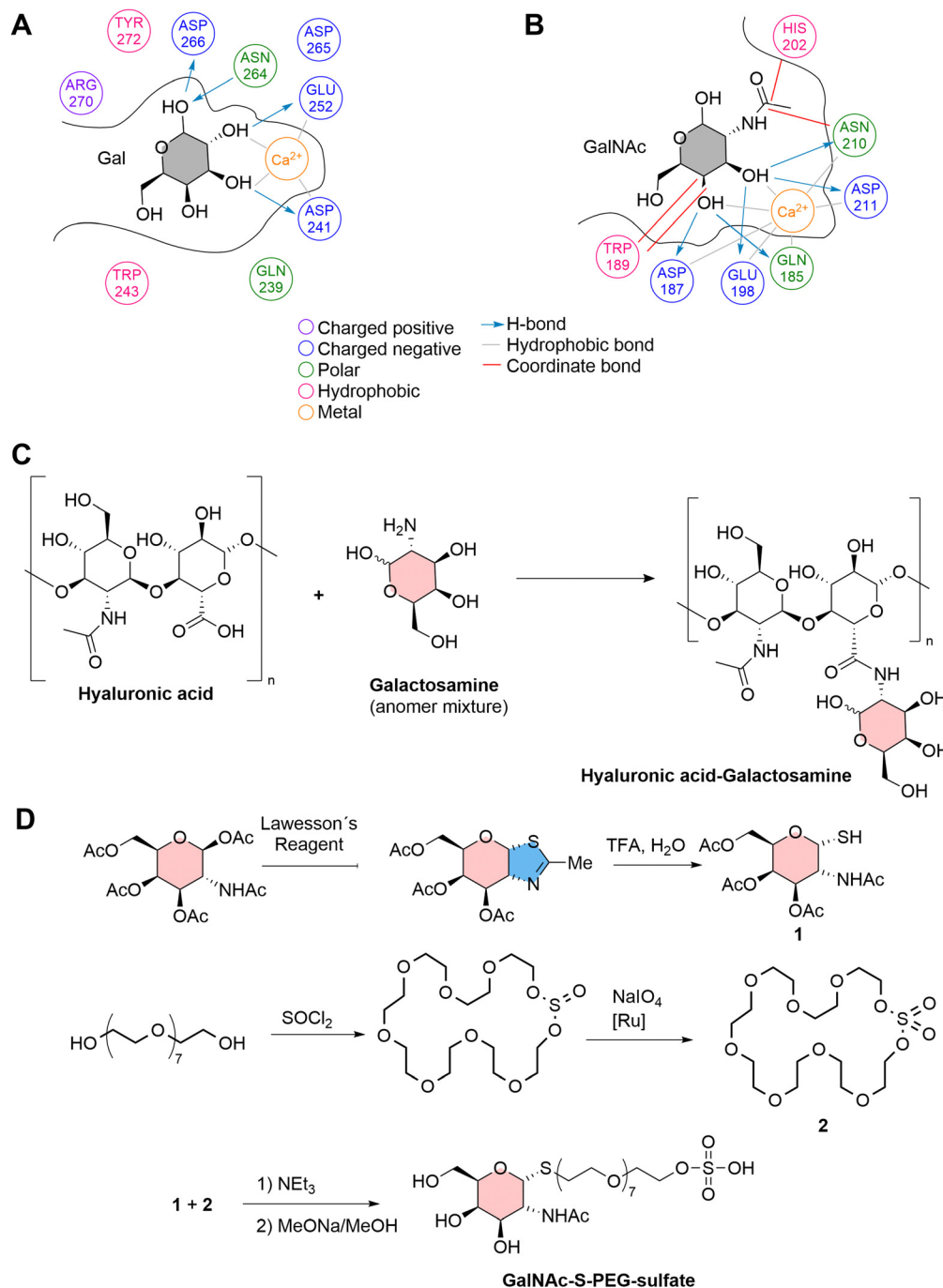


Fig. 5 Molecular interactions between (A) galactose, and (B) *N*-acetyl-galactosamine (GalNAc) at the active binding site (CRD) of ASGPR. (C) The preparation of HA-galactosamine for the functionalization of CaCuMOF.<sup>77</sup> (D) Synthetic strategy for the preparation of a ligand based on *N*-acetylgalactosamine and sulphated PEG for the functionalization of PCN-222.<sup>11</sup>

these examples, no chemical modification of the monosaccharides was performed (except for those required to link them to the MOFs), nor were any specific spacers used between the monosaccharide and the MOF. This limitation affects targeting capabilities. For instance, in the case of targeting the ASGPR, it has been demonstrated that the structural characteristics of the

monosaccharides are critical for interaction with the C-terminal carbohydrate recognition domain (CRD) of ASGPR. Specifically, the CRD of ASGPR comprises the amino acids aspartic acid 241, aspartic acid 265, asparagine 264, glutamic acid 252, glutamine 239, and tryptophan 243.<sup>78</sup> CHS binding is initiated by the coordination of specific amino acids in the



receptor with  $\text{Ca}^{2+}$  ions, facilitating the binding of hydroxyl moieties (Fig. 5(A)). The binding of ASGPR ligands is influenced by several factors including the proximity of  $\text{Ca}^{2+}$  to two oxygen atoms (preferably the 3-OH and 4-OH groups) of the sugar, which allows for coordinate bond formation, the orientation of the pyranose ring of the sugar to maximize hydrophobic interactions between tryptophan 243, and the carbon atoms of the ligands (C3–C6), and numerous hydrogen bonds that stabilize ligands at the binding site.<sup>78</sup> As shown in Fig. 5(B), this binding is particularly enhanced when using specifically designed CHs, such as *N*-acetyl-galactosamine.

For example, in a recent study, a polyethylene glycol (PEG) ligand was synthesized with thio-*N*-acetyl-galactosamine linked through C1 at one end and a sulfate group at the other end. This ligand was then attached to PCN-222 through interactions between the sulfate group and Zr nodes, utilizing a continuous flow reactor. The presence of a spacer with specific length allowed avoiding steric hindrance limitations, leaving the external *N*-acetyl-galactosamine free to potentially interact with ASGPR with enhanced interactions compared with pure galactosamine (Fig. 5(D)).<sup>11</sup>

In another peculiar investigation, the possibility of using amphiphiles for the functionalization of hydrophobic MOFs, rendering water-dispersible nanosystems, was also explored. This strategy has been employed for the stabilization of ZIF-8, a hydrophobic MOF,<sup>79</sup> which after incubation with an alkyl-polyglucoside such as *n*-dodecyl  $\beta$ -D-maltoside, gives rise to water-dispersible micelles (Fig. 6(B)).<sup>80</sup> This glyco-MOF nanosystem contains maltose-exposing sugar moieties, and this strategy can thus be used to obtain colloidal suspensions of nonpolar nanoparticles in polar solvents.<sup>33,57,75,77</sup>

Aiming at establishing more robust CH-MOF interactions, researchers also explored bioconjugation reactions, sometimes referred as to grafting. CHs-MOFs prepared by bioconjugation show the advantage of enhanced thermal and mechanical resistance. For example, hyaluronic acid (HA), a nonsulfated GAG, has been conjugated with a ZIF-8 derived nanostructure which contains hydrophilic carboxylic acid groups in the MOF

organic linkers. Standard EDC/NHS chemistry (*i.e.*, the formation of amide bonds from carboxyl and amine groups) was employed, resulting in the synthesis of HA/FZIF-8 films with antibacterial properties.<sup>82</sup> With another approach, MIL-101(Fe) surfaces were functionalized with the GAG heparin, normally used as an anticoagulant agent, to enhance colloidal stability across various biological environments.<sup>83</sup> The heparin-functionalized MIL-100(Fe) (HP-on-MIL-100(Fe)) exhibited a drug loading capacity reaching up to 42 wt% using caffeine as a model drug. Additionally, HP-on-MIL-100(Fe) provided superior control over the drug release compared to the uncoated MIL-100(Fe). A similar strategy has been reported for the incorporation of galactose and mannose to the  $\text{NH}_2$ -MIL-53(Fe) surface. This MOF contains 2-aminoterephthalic acid ( $\text{NH}_2$ -BDC) linkers, which are used for the conjugation with 4-aminophenyl- $\beta$ -D-galactopyranoside and 4-aminophenyl- $\alpha$ -D-mannopyranoside after the MOF synthesis, in the presence of glutaraldehyde. The authors eventually obtained a glyco-MOF with applications in the sensing and detection of bacteria.<sup>84</sup> Analogously,  $\text{NH}_2$ -MIL-101(Fe) nanoparticles treated with hyaluronic acid in the presence of EDC result in a hybrid HA-on-MIL nanosystem in which the  $-\text{COOH}$  groups of polysaccharides and the  $-\text{NH}_2$  groups of the MOF form an amide bond. In particular, this carrier can be loaded with platinum-based drugs for targeted cancer therapy (Fig. 6(A)).<sup>81</sup> The  $\text{NH}_2$ -MIL-101 MOF can also be suitable for click chemistry conjugation. For example, a first conversion of the amino to an azide group followed by a reaction with 1-propargyl-*O*-maltose gave rise to a maltose-on-MOF with applications in the fast determination of small biomolecules.<sup>85</sup>

Similarly,  $\text{NH}_2$ -UiO66 was functionalized with D-mannose by reductive amination using sodium triacetoxyborohydride as the reducing agent,<sup>86</sup> and sequentially the recombinant human bleomycin hydrolase (rhBLMH) was encapsulated. When the resulting nanosystems were administered intratracheally, the nanoparticles entered epithelial cells, protecting the lungs from pulmonary fibrosis during bleomycin-based chemotherapies. Encapsulating rhBLMH in MHP-UiO-66 also shielded the enzyme from proteolysis and improved cellular uptake.

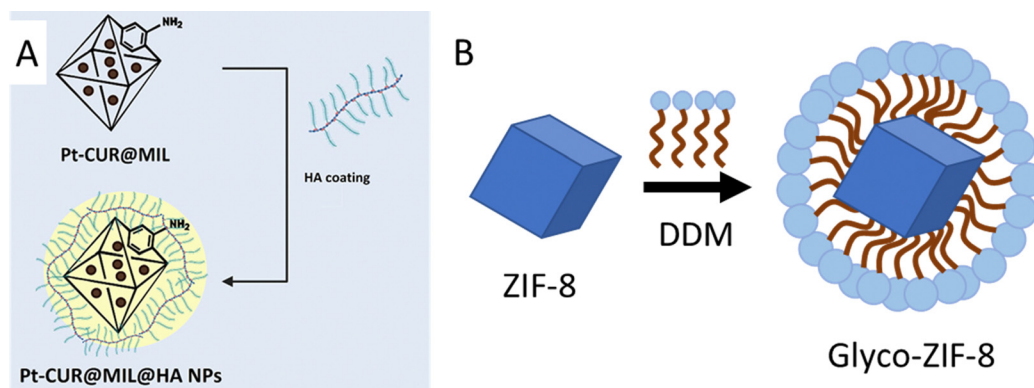


**Fig. 6** (A) Conjugation of platinum-curcumin ( $\text{NH}_2$ -MIL-101(Fe)) nanoparticles and hyaluronic acid. Amino groups belonging to the ligand 2-aminoterephthalic acid react with  $-\text{COOH}$  groups of hyaluronic acid, in the presence of EDC/NHS. Taken from ref. 81 and reproduced with permission from John Wiley & Sons Ltd, copyright 2022. (B) Functionalization of ZIF-8 NPs with the amphiphile *n*-dodecyl  $\beta$ -D-maltoside (DDM), resulting in water-dispersible glyco-ZIF-8 micelles exposing carbohydrate moieties. Adapted from ref. 80 published by the American Chemical Society, copyright 2019.



Table 2 Selected publications related to CHs-MOFs prepared by PSM

CHs	MOF	Role of CHs	Aim of CHs-MOFs	Ref.
Heparin	MIL-101(Fe)	Anticoagulant for PTFE implant	Controlled release of heparin during degradation	71
Heparin	MIL-100(Fe)	Evasion from the recognition by immune cells	Controlled release of caffeine (model drug) and furazan-derivate (antitumoral)	83
Heparin	Fe-MOF	Increase the accumulation and luminescent intensity	Piezoelectric-Fenton-photodynamic images (theragnostic)	88
Hyaluronic acid	ZIF-8	Antibacterial properties	Wound healing applications	82
Hyaluronic acid	MIL-100(Fe)	Targeting of cancer cells	Delivery of indocyanine green for photothermal therapy	66
Hyaluronic acid	PCN-224	Increase biocompatibility, act as polymer gatekeeper and targeting cancer cells	Controlled release of doxorubicin and photodynamic therapy	51
Hyaluronic acid	PCN-224	Targeting of cancer cells	Controlled release of immunologic adjuvant (CpG) and photodynamic therapy	65
Hyaluronic acid	ZIF-8	Increase the biocompatibility, stability and targeting of cancer cells	Controlled release of chlorin e6 for photodynamic therapy	67
Hyaluronic acid	ZIF-8	Targeting of cancer cells	Controlled release of doxorubicin	70
Hyaluronic acid	MIL-101(Fe)	Increase cellular uptake	Controlled release of 5-fluoroacil (anticancer)	89
Hyaluronic acid	ZIF-8	Negative charge of the MOFs for use on contact lenses and biocompatibility	Controlled release of levofloxacin (antibacterial)	90
Hyaluronic acid	Cu/PCN-224	Improve water dispersibility and biocompatibility	Controlled release of disulfiram prodrug (anticancer)	91
Hyaluronic acid	ZIF-8	Improve the stability	Controlled release of evodiamine (anticancer)	92
Hyaluronic acid	UiO-66	Increase stability and cellular uptake	Controlled release of 5-fluoroacil (anticancer)	93
Hyaluronic acid	Fe/Cu-MOF	Increase stability and cellular uptake	Controlled release of lactate oxidase and Fe/Cu for chemodynamic therapy	94
Hyaluronic acid	Zr-MOF	Targeting of cancer cells	Photo dynamic therapy	68
Hyaluronic acid	Fe-MOF	Targeting of cancer cells	Photo dynamic therapy	69
Hyaluronic acid	MIL-101(Fe)	Increase stability and biocompatibility	Controlled release of platinum-curcumin	81
Hyaluronic acid	ZrTc MOF	Targeting of cancer cells	Hydrogen therapy	95
Hyaluronic acid	ZIF-8	Targeting of cancer cells	Controlled release of cisplatin (CDDP) and SR-717 (a STING agonist)	96
Hyaluronic acid	Ag <sub>2</sub> S/ZIF-8	Targeting of cancer cells	Controlled release of doxorubicin and photodynamic therapy	97
Hyaluronic acid	Fe-MOF	Targeting of cancer cells	Controlled release of L-buthionine sulfoximine (BSO) and chlorin e6 for photodynamic therapy	98
Hyaluronic acid	Fe-MOF	Targeting of cancer cells	Controlled release of Fe (Fenton reaction), oxaliplatin and L-arginine	99
Hyaluronic acid (sulfonated)	Cu-MOF	Anticoagulant and anti-inflammatory	Improve the biocompatibility of implant materials.	100
Galactosamine-linked hyaluronic acid	CaCu-MOF	Increase stability	Controlled release of doxorubicin and Cu for chemodynamic therapy	77
Carboxymethyl-dextran	MIL-100(Fe)	Increase stability and biocompatibility	Controlled release of daunorubicin (anticancer)	73
Phosphated cyclodextrins	MIL-100(Fe)	Increase stability	Potential drug delivery system	29
Carboxymethylcellulose	Cu-MOF	Increase stability in PBS	Controlled release of ibuprofen	74
Carboxymethylcellulose	UiO-66-NH <sub>2</sub>	Increase stability in PBS	Controlled release of 3,4-dihydroxybenzaldehyde (DHBD) drug and 5-fluorouracil	101
Chitosan-graft-poly (lactic acid)	CD/MOF	Increase solubility	Controlled release of curcumin (as a model water insoluble drug)	102
Chitosan	MIL-100 (Fe)	Increase resistance to degradation	Controlled release of piperine (anticancer)	103
Chitosan	Cu-MOF	Increase biocompatibility	Controlled release of doxorubicin (anticancer)	104
Chitosan	Ca-MOF	Increase biocompatibility	Controlled release of Ca and alendronate for bone engineering	105
Chitosan	MOF-808	Improve stability	Controlled release of quercetin (QU)	75
Cellulose/chitosan	MOF-199	Support media for MOF	Extraction of benzodiazepines (BZPs) from urine	106
B-cyclodextrin	MOF-235	Increase luminescent intensity	Glucose detection in human serum	107
D-Mannose	Fe-MOF	Targeting of cancer cells	Controlled release of doxorubicin and methotrexate	108
D-Mannose	MIL-100(Fe)	Targeting of cancer cells	Applications for chemodynamic therapy (CDT)	76
D-Mannose	UiO-66	Targeting of cancer cells	Controlled release of recombinant human bleomycin hydrolase (rhBLMH) to prevent pulmonary fibrosis	86
Mannosamine	MIL-88A(Fe)	Targeting of cancer cells	Internalization in alveolar macrophages	109
D-Mannose (poly(acrylic acid-mannose acrylamide))	MIL-100(Fe)	Targeting of cancer cells	Controlled release of both carboplatin and floxuridine	27
Glucose	Gd-MOFs	Increase biocompatibility, act as gatekeeper and targeting cancer cells	Controlled release of doxorubicin	72



Table 2 (continued)

CHs	MOF	Role of CHs	Aim of CHs-MOFs	Ref.
Galactose and mannose	MIL-53(Fe)	Targeting receptors of bacteria	Detection of <i>P. aeruginosa</i> and <i>E. coli</i>	84
Galactose	PCN-224	Targeting of cancer cells	Controlled release of doxorubicin and photodynamic therapy	87
Galactose	ZnAP-MOF	Targeting of cancer cells	Controlled release of 6-allylthiopurine (6-AP)	110
<i>N</i> -Acetylgalactosamine	PCN-222	Targeting of cancer cells	Potential drug carrier and photodynamic therapy	11
Maltose ( <i>n</i> -dodecyl $\beta$ -D-maltoside)	ZIF-8	Stability and potential targeting	Potential drug carrier	80
Maltose	MIL-101	Ultrahigh ionization efficiency, free matrix background, uniform crystallization, and good dispersibility	Determination of small biomolecules by laser desorption ionization mass spectrometry (LDI-MS)	85

The nanoparticles also boosted pulmonary accumulation of rhBLMH, offering more effective lung protection during chemotherapy.

A combination of bioconjugation and the formation of weaker interactions has been employed for the incorporation of galactose to the PCN-224 surface. In the first step, after the MOF synthesis, the NPs were coated with polyethylene glycol with carboxylate terminals (COOH-PEG-COOH) through electrostatic adsorption. These NPs thus exhibited –COOH on their surface, which reacted with amine-modified galactose in the second step, using ethyl-(dimethylaminopropyl)carbodiimide (EDC) as a coupling agent. This hybrid nanosystem was used for the targeted photodynamic and chemotherapy therapy of hepatocellular carcinoma.<sup>87</sup> A relatively high number of other studies have reported novel CHs-MOFs systems prepared by PSM. Some of the most recent and relevant are reported in Table 2.

**Incorporation of CHs during the synthesis of MOFs.** The encapsulation of carbohydrates by MOFs, the so-called CH@MOF structures, are usually employed to preserve the biological activity of biomolecules,<sup>111</sup> avoiding also their leaching before reaching the site of action (in the context of nanoparticles, “@” is commonly used to denote a core-shell structure or encapsulation, where one material – normally the first one in order – is coated or surrounded by another – the one after the @). Analogously to other biomolecules, CH and CH-based drugs can be encapsulated into the cavity of the MOFs, producing in many cases structurally stable host-guest ensembles. To date, this strategy has been limited to few polysaccharides, such as HA, chondroitin sulfates, dermatan sulfates, keratin sulfates and heparan sulfates. Recently, glycosaminoglycans (GAG) containing heparin (HP), HA, chondroitin sulfate (CS), and dermatan sulfate (DS) were also encapsulated in Zn-azolate frameworks ZIF-8, ZIF-90, and MAF-7 through a one-pot strategy, resulting in GAG@MOF biocomposites. The hybrid CH@MOF nanostructures were synthesised in aqueous solutions from their Zn precursors and the corresponding ligands in the presence of the carbohydrates (Fig. 7(A)).<sup>112</sup>

Carboxylate-functionalized dextran has also been encapsulated into ZIF-8 pores. The modified polysaccharide was used as biomimetic mineralisation agents for the formation of CHs@ZIF-8 biocomposites, and was also added to the reaction media during the MOF synthesis. It should be noticed that the presence of carboxylate functional groups was identified as a key factor for successful encapsulation<sup>113</sup> of the polysaccharide, and that the encapsulation of monosaccharides or

oligosaccharides such as D-glucose, D-galactose, D-mannose D-xylose and sucrose was not possible (Fig. 7(B)).<sup>114</sup> Table 3 summarises other recent examples of CHs@MOFs, while a list of more dated works can be found elsewhere.<sup>35</sup>

Another approach for the preparation of CHs-MOFs by incorporating the CHs during the synthesis of MOFs, exploits the presence of reactive chemical groups of CHs capable of coordinating with inorganic metals. This approach has already resulted in different types of MOFs using lipids, proteins, and nucleic acids, but has attracted less attention and technical challenges with CHs. Currently, researchers have achieved crystalline MOFs practically only employing cyclodextrins (CD). Among most methods used for the preparation of CD-MOFs, researchers have investigated vapor-diffusion, solvothermal, liquid-liquid methods, and microfluid synthesis. Recently, CD-MOFs based on  $\gamma$ -CD were prepared by an ultrasonic-assisted solvothermal method, obtaining uniformly-sized nanoscale edible NPs, avoiding the issue of poor size distribution, one of the most common problems of CD-MOFs.<sup>116</sup> The NPs were further modified by ester bond cross-linking, to obtain a nanosystem capable of loading quercetin, a naturally occurring flavonoid bioactive compound, that has antioxidant, anti-inflammatory, and anticancer effects. The CD-MOF showed storage stability for 14 days, and enhanced biocompatibility. CD-MOFs were also prepared using a stream diffusion method using green chemistry principles, followed by loading with apigenin, a potential bioactive functional food ingredient.<sup>117</sup> As mentioned in the introduction, reviews related to CD-MOFs and recent trends in this field have already been reported in the literature and are not here repeated.<sup>26,45–47</sup> Another strategy that can be somehow classified as a type of methodology using CHs as building units, is the use of CHs as a sort of template for the controlled growth of MOFs. This is the case in the preparation of HKUST-1 and ZIF-8 with chitosan,<sup>114</sup> and some examples in which fructose is used as the MOF organic linker in Sr<sup>2+</sup> and Ca<sup>2+</sup> based MOFs have also been reported in the literature.<sup>119,120</sup> However, in general, the preparation of CHs-MOFs using CHs during the synthesis of MOFs is less explored to date and, especially in the case of using CHs as building units, practically limited to the use of CDs, as summarized in Table 3.

## Advancements in preclinical evaluations of CHs-MOFs

Over the past few years, some different CHs-MOFs have already been tested in preclinical trials. While their application in



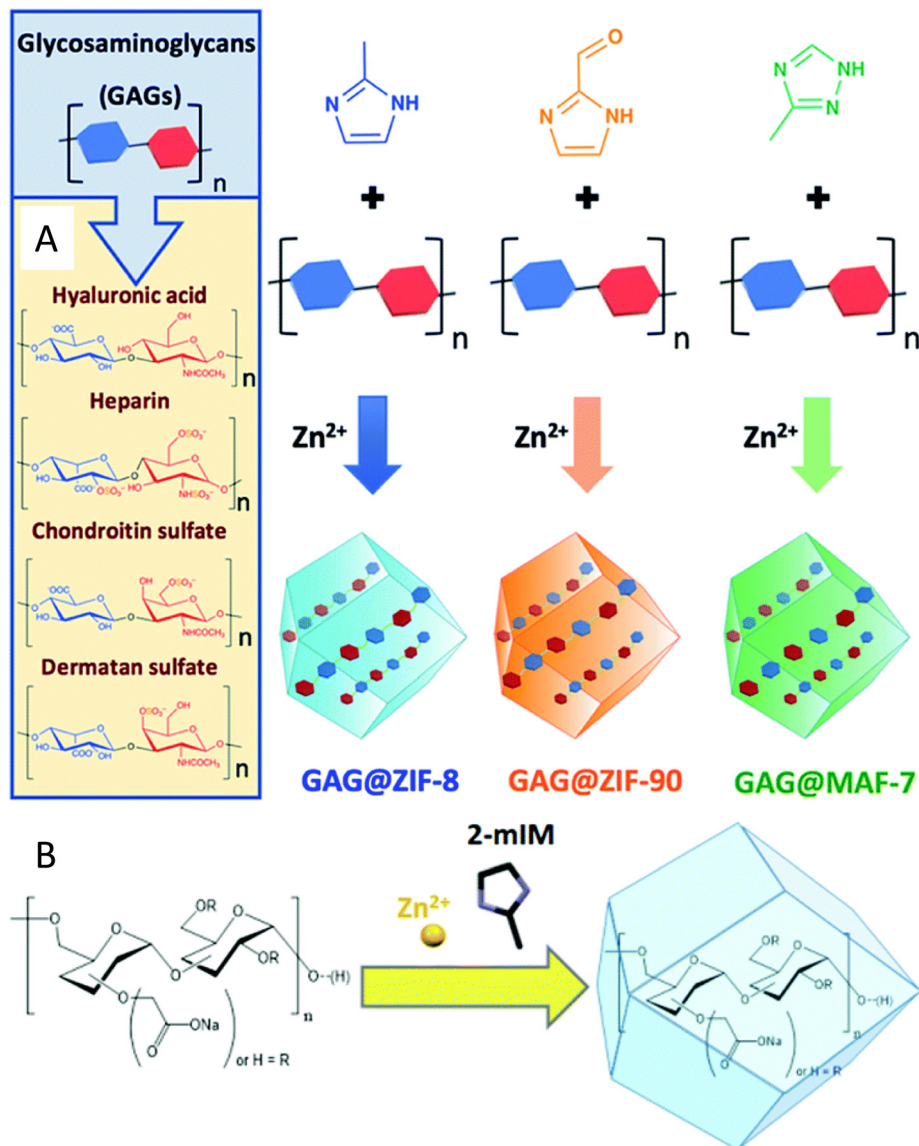


Fig. 7 Encapsulation of carbohydrates (polysaccharides) in MOF pores. (A) One-pot synthesis of glycosaminoglycans GAG@MOF biocomposites based on three different metal-azolate frameworks. Taken from ref. 112 published by the Royal Society of Chemistry. (B) Biomimetic mineralisation of carboxylated-dextran@Zn(2mIM)<sub>2</sub>. In both cases the MOFs are synthesised from their metal precursor and organic ligands in the presence of the carbohydrates. Taken from ref. 113 published by the Royal Society of Chemistry.

industrial settings still requires further validation, these trials have confirmed their potential for biomedical use. One notable example is MIL-100(Fe), engineered specifically to co-deliver oxaliplatin (OXA)—a widely used platinum-based chemotherapy drug for advanced colorectal cancer (CRC)—and *L*-arginine (*L*-Arg) to combat OXA resistance (Fig. 8(A)).<sup>99</sup> The synthesis of the MOF involved encapsulating both OXA and *L*-Arg within its porous structure, followed by surface modification with hyaluronic acid, facilitating binding to CD44 receptors. This resulted in the formation of the *L*-Arg&OXA@MOF-HA construct. Upon reaching the tumour site, the high levels of glutathione (GSH) characteristic of the tumour microenvironment reduce Fe<sup>3+</sup> to Fe<sup>2+</sup>, leading to the disintegration of the MOF structure and the controlled release of OXA and *L*-Arg.

This mechanism not only depletes intracellular GSH but also augments the cytotoxic efficacy of OXA. Furthermore, the released Fe<sup>2+</sup> initiates a Fenton reaction with endogenous hydrogen peroxide, generating hydroxyl radicals and liberating nitric oxide (NO). This cascade of reactions collectively sensitizes cancer cells and induces cell death through oxidative stress. *In vitro* experiments (Fig. 8(B)) demonstrated a significant enhancement in cytotoxicity against OXA-resistant HCT-116/L colorectal cancer cells, achieving more than 60% reduction in cell viability compared to treatment with OXA alone. Flow cytometric analysis confirmed an increase in apoptosis, with elevated levels of reactive oxygen species and NO detected in the treated cancer cells. *In vivo* studies utilizing tumour-bearing mice exhibited marked tumour inhibition,



Table 3 Selected publications related to CHs-MOFs prepared by using CHs during the synthesis of MOFs

CHs	MOF	Role of CHs	Aim of CHs-MOFs	Ref.
Encapsulated CHs				
Different polysaccharides	ZIF-8	Biomimetic mineralisation and therapeutics	Controlled release of polysaccharide-based therapeutics	113
Glycosaminoglycans (GAGs)	ZIF-8 ZIF-90 MAF-7	Therapeutics	Controlled release of GAGs	112
Fuoidan	EuMOF	Therapeutic	Controlled release of fuoidan	115
CHs as building units				
Chitosan	HKUST-1 ZIF-8	Control the biomimetic growth of MOFs	Demonstrate the polysaccharides are an excellent medium for the growth and the expansion of crystalline MOFs	114
$\gamma$ -CD	CD-MOF	Biocompatibility	Controlled release of quercetin (dietary supplement)	116
B-CD	CD-MOF	Biocompatibility	Controlled release of apigenin (dietary supplement)	117
Fructose	Sr-based MOF	Coordinate Sr ions	Promotes the encapsulation of earth alkaline ions on chitosan NPs	118

with the group treated with the CHs-MOFs showing the most pronounced tumour suppression. Notably, the nanoplatform exhibited high biocompatibility, with negligible toxicity recorded in healthy human liver cells (HL-7702) and macrophages.

In another study, UiO-66-NH<sub>2</sub> was modified *via* a Schiff base reaction with 4-dihydroxybenzaldehyde (DHBD) forming a pH-sensitive C=N bond.<sup>101</sup> This MOF was subsequently encapsulated within a hydrogel matrix composed of carboxymethyl cellulose (CMC) and alginate, yielding a dual pH-responsive delivery system designed to co-deliver DHBD@MOF and 5-fluorouracil (5-FU) for colorectal cancer therapy. The CMC coating effectively protects the drug from premature release in acidic environments such as the stomach and small intestine, facilitating the release of active agents in the neutral to slightly acidic pH of the colorectum. Preclinical release studies demonstrated that only 1.31% of DHBD was released from the hydrogel at pH 1.2 (simulating stomach acid) within 2.5 hours, thereby preventing premature drug degradation. Under tumour-like conditions at pH 6.5–7.4, however, a controlled and sustained release was achieved, with significant drug release observed over 8.5 and 24 hours. Specifically, 41.68% of the drug was released after 24 hours in the acidic microenvironment typical of colorectal cancer, with 89.40% and 58.32% of the inactive DHBD@MOF prodrug infiltrating the tumours after 8.5 hours and 24 hours, respectively. In pursuit of a similar pH-responsive strategy, FU@Eu-MOF was developed to enhance drug delivery for lung cancer therapy.<sup>115</sup> Fuoidan (FU), a bioactive polysaccharide, was encapsulated within a europium-based MOF through a one-pot synthesis. *In vitro* studies indicated that FU@Eu-MOF significantly improved cytotoxicity against A549 lung cancer cells compared to free fuoidan or Eu-MOF alone. This system achieved a high drug loading efficiency of 22.15% by weight and exhibited a controlled release profile (85.3% over 48 hours), particularly in acidic environments (pH 5–6), which mimic tumour tissues. The results demonstrated that FU@Eu-MOF exhibited enhanced anticancer potential, with an IC<sub>50</sub> value of approximately 32  $\mu\text{g ml}^{-1}$ , compared to fuoidan alone, which had an IC<sub>50</sub> value of approximately 60  $\mu\text{g ml}^{-1}$ . This improvement is attributed to the combination of elevated reactive oxygen species (ROS) levels leading to DNA damage and mitochondrial dysfunction-mediated apoptosis. Specifically, the extent of ROS-mediated DNA damage was

assessed in terms of the percentage of tail DNA. Vehicle control cells exhibited *ca.* 97% head DNA with only 3% tail DNA. In contrast, FU@Eu-MOF and fuoidan-treated cells showed approximately 31% head DNA and 10% tail DNA, respectively. Additionally, apoptotic cell rates in the FU@Eu-MOF and fuoidan-treated groups were recorded at approximately 82% and 48%, respectively, in contrast to only about 5% apoptotic cells in the vehicle control group (Fig. 9(A)).

Another CHs-MOFs was developed utilizing the purine nucleobase prodrug, 6-allylthiopurine (6-ATP), in conjunction with a ZnAP MOF to enhance synthetic lethal therapy in cancer treatment.<sup>110</sup> Prodrug-skeletal MOFs (ZnAP) were synthesized through a solvothermal method employing 6-AP, biphenyl-4,4'-dicarboxylic acid (4-BPA), and Zn<sup>2+</sup>. The PARP inhibitor (ANI) was conjugated with a hydrophilic chain terminated with galactose *via* an amide linkage to yield Gal-ANI, which exhibits aggregation-induced emission (AIE) to facilitate monitoring of drug uptake. Subsequently, Gal-ANI was modified onto the surface of ZnAP *via*  $\pi$ - $\pi$  stacking and hydrogen bond interactions, culminating in the construction of Gal-ANI-on-ZnAP. The incorporation of a glycosylated AIE PARP inhibitor enabled real-time visualization of drug uptake in cancer cells. *In vitro* studies revealed pH and esterase responsiveness of Gal-ANI-on-ZnAP, with 86% of ANI and 88% of 6-AP released at pH 5.0 in the presence of esterase after 48 hours, thereby minimizing toxicity to healthy cells. Fluorescence studies confirmed effective uptake of the NPs in HepG2 cells, attributed to their affinity for the asialoglycoprotein receptor (ASGPR). In contrast, negligible fluorescence was observed in HL7702 cells, which exhibit low ASGPR expression, indicating targeted delivery. Cytotoxicity assays revealed that Gal-ANI-on-ZnAP NPs were highly toxic to HepG2 cells, achieving only 13% survival at a concentration of *ca.* 90  $\mu\text{g ml}^{-1}$  after 48 hours, while HL7702 cells maintained over 75% viability, highlighting the selective antitumor activity of the NPs. Colony formation assays further illustrated their significant antiproliferative effects. Furthermore, treatment with Gal-ANI-on-ZnAP resulted in a decreased mitochondrial membrane potential (MMP) and elevated reactive oxygen species (ROS) levels in HepG2 cells, signalling the induction of apoptosis. Flow cytometry analysis demonstrated a substantial apoptosis rate of 97.27% in treated cells,



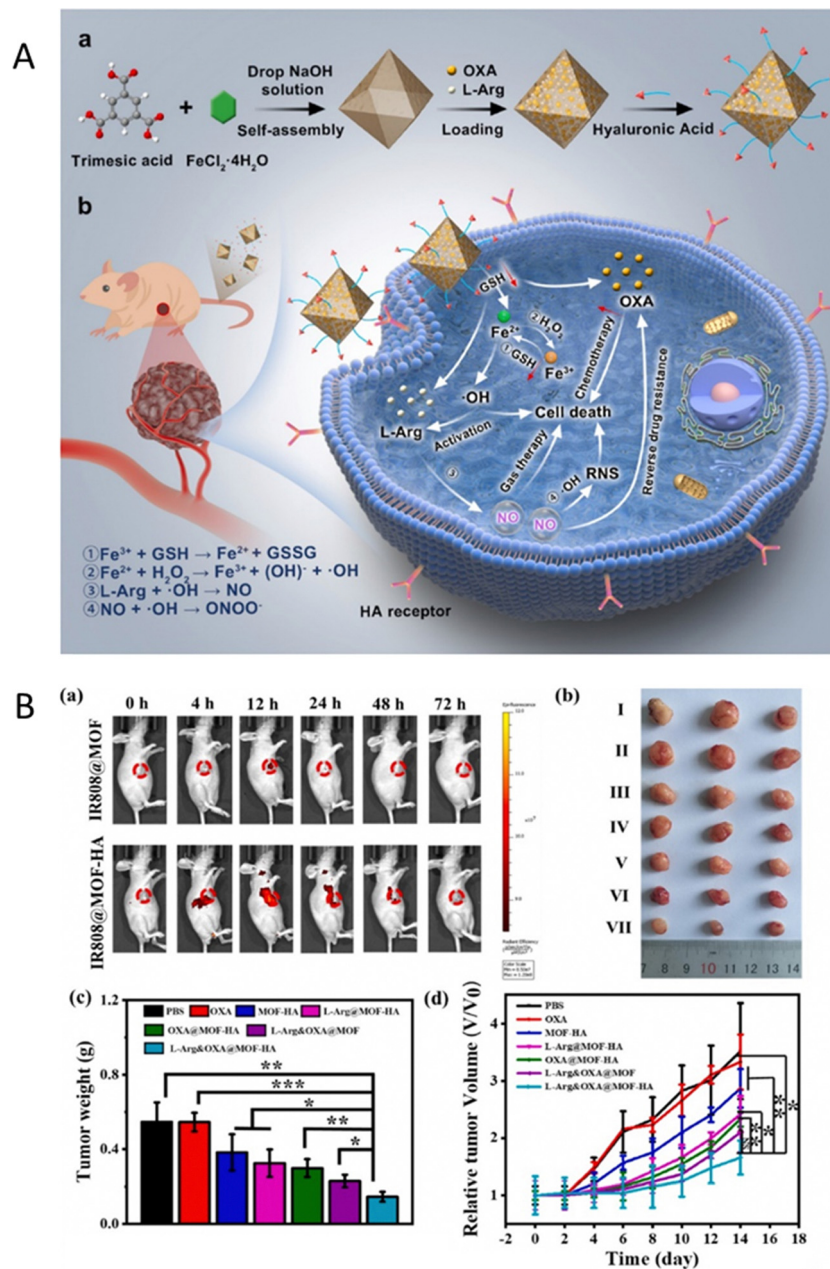


**Fig. 8** (A) (a) Preparation process of the designed nanoplatform; (b) potential mechanisms by which the nanoplatform overcomes drug resistance and exerts anti-CRC effects. (B) (a) Time-dependent *in vivo* imaging of HCT-116/L tumor-bearing mice administered MOFs *via* intravenous injection; (b) photographs of tumours from mice following indicated treatments (I: PBS; II: OXA; III: MOF-HA; IV: L-Arg@MOF-HA; V: OXA@MOF-HA; VI: L-Arg&OXA@MOF; VII: L-Arg&OXA@MOF-HA); (c) average tumour weights across treatment groups; (d) tumour growth profiles for mice receiving the indicated treatments. Scale bars represent 50  $\mu\text{m}$ . Reprinted and adapted from ref. 99 with permission from Elsevier, copyright 2024.

attributed to DNA damage resulting from the combined effects of ANI and 6-AP.

## Conclusions and outlook

The integration of carbohydrates into metal-organic frameworks (MOFs) creates CHs-MOFs composites exhibiting synergistic properties such as enhanced chemical and thermal stability, controlled release, and higher selectivity, which are

not observed in the individual components. Additionally, incorporating CHs into MOFs can improve the bioavailability and pharmacokinetics of carbohydrate-based therapeutics. These hybrid nanosystems have potential applications as drug delivery systems, analytical tools, and can also serve as contrast agents for imaging techniques like magnetic resonance imaging (MRI) and computed tomography (CT). The increasing number of research articles and patents highlights the growing interest and significant industrial investment in this field. For instance, CN110545793B discusses a method for preparing



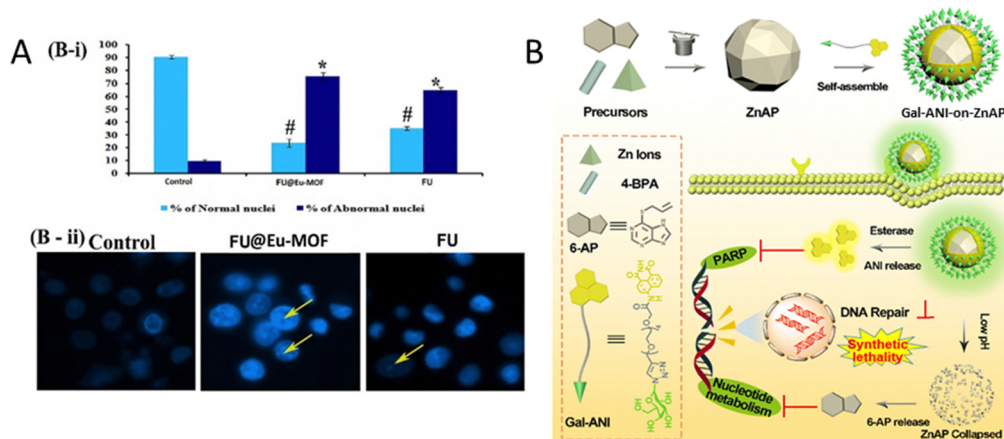


Fig. 9 (A) B: Alterations in nuclear DNA: (i) quantitative results for the number of apoptotic cells per 100 total cells, (ii) microscopic images illustrating nuclear fragmentation, DNA nicks, and nuclear deformities. Reprinted and adapted from ref. 115 with permission from Elsevier, copyright 2022. (B) Schematic illustration of the construction of Gal-ANI-on-ZnAP and its application for synthetic lethal therapy and visualization therapy adapted from ref. 110.

MOFs modified with specific ligands, including hyaluronic acid, to target CD44 receptors in tumour cells. Similarly, CN108187046B reports a MOF shielded with hyaluronic acid that can carry curcumin for both cancer diagnosis and treatment. Some other patents are related to CD-MOFs, such as US10583147B2, US9085460B2, CN107151329B, and CN107837401B. For example, US10125016B2 reports a method for the environmentally friendly synthesis of CD-MOFs, and US10500218B2 describes loading different drugs into CD-MOFs for biomedical applications.

However, despite the tremendous potential of CHs-MOFs and the burgeoning focus in the field, many challenges and limitations must be addressed to shift academic R&D results to real-world biomedical applications:

1. Scalability and reproducibility: firstly, substantial technical challenges related to the large-scale preparation of MOFs for biomedical applications need to be addressed. This includes achieving good reproducibility and yields of size-controlled MOF nanoparticle synthesis. These challenges are compounded by the poor understanding and modelling of MOF crystallization, from seed formation to growth.<sup>121</sup> Currently, most MOF-related papers are limited to synthesizing only dozens of milligrams or few grams per batch, and larger-scale productions are rarely considered,<sup>122,123</sup> and are practically unreported for biomedical applications.<sup>124</sup> This limitation should also be addressed when using intensified processes, such as continuous flow synthesis, as well as other innovative technologies like microwave and ultrasound-assisted synthesis, which are typically explored for their potential to scale-up but rarely demonstrated effectively for this purpose.<sup>125,126</sup> Reaching reliable, large-scale production methods is essential for translating CHs-MOFs from research to clinical applications.

2. Size control: achieving precise control over the size of CHs-MOFs is difficult, as size distribution is often influenced by kinetic factors, which are harder to scale up than thermodynamic control. Many studies in the literature do not address the size distribution of the produced CHs-MOFs, and only a few have investigated how various experimental conditions impact

their shape and size. For example, the first study on the effect of the different parameters on the shape and size of PCN-222 was only recently reported.<sup>11</sup> Furthermore, as mentioned earlier, the impact of the size of CHs-MOFs on ADMET should be thoroughly explored, potentially using advanced computational techniques such as machine learning (ML).

3. Sustainability characteristics: the sustainable production of MOFs should be considered, as current preparation methods are typically energy and solvent-consuming. For example, MIL-101(Fe) and PCNs are produced using DMF (*N,N*-dimethylformamide),<sup>125,126</sup> a highly toxic and potentially carcinogenic solvent. Although some articles have recently discussed environmentally friendly MOF synthesis for biomedicine, opening the research to this type of investigation, requires much more effort, including green metrics<sup>127–129</sup> and life cycle assessment (LCA) calculations.<sup>130</sup> At the same time, the well-established chemistry of carbohydrates and the production of CH-based drugs, considering the green principles of chemistry, is an advantageous point in developing CHs-MOFs. However, only a few monosaccharides have been exploited to produce CHs-MOFs, with polymeric CHs being more commonly selected. This implies limited chemical control, and the effect of different sizes of CH-polymers on bio-interactions within CHs-MOFs is not well understood.<sup>131</sup> Natural ligands should also be more extensively considered as tools for functionalizing MOFs with CHs, as demonstrated recently with a lecithin-based ligand used for the functionalization of MOFs with D-mannose.<sup>132</sup>

4. Biological interactions between CHs and MOFs: the synergy between CHs and MOFs in biological systems remains poorly understood. Investigating how these two components interact, both at the molecular level and within living organisms, is crucial for maximizing their therapeutic efficacy and ensuring their safe use. These interactions influence key factors such as targeting capabilities, biodegradability, and long-term stability in biological environments. Therefore, significant effort is required to investigate bio-CHs-MOFs interactions and design more appropriate and efficient systems, including



specifically-modified CHs for targeting, and precise linkers/spacers for the modification of MOFs, similarly to what is carried out with other types of NPs.<sup>57,133,134</sup> This will require an interdisciplinary approach, combining expertise from materials chemistry, organic chemistry, biology, and computational chemistry. While this approach is still largely unexplored, it has great potential for advancing the field.

In addition, there are specific limits related to the different methods used to prepare the CH-MOFs, that needs to be implemented. In particular:

- CHs-on-MOFs prepared through PSM by low/medium energy interactions. This simple technique avoids harsh conditions and complex synthetic procedures but results in less stable CHs-MOFs. However, CHs may be less stable than covalently linked ones, leading to leaching and decreased bioactivity over time. The process may also be less efficient due to a limited number of reactive sites, resulting in lower surface coverage and heterogeneous distribution of carbohydrates, leading to non-uniform properties.

- CHs-on-MOFs prepared through PSM by bioconjugation. CHs-MOFs produced this way are more stable, and it is easier to control the location of CHs within the MOF structure. This method offers versatility due to the wide range of available MOFs and various methods for modifying MOF surfaces. Despite these strengths, grafting presents challenges, such as ensuring covalent bond formation does not disrupt the MOF structure or compromise its properties. The synthesis process is often more complicated and time-consuming, requiring precise control over reaction conditions and purification methods.

- CHs@MOFs prepared *via* encapsulation. This method results in more durable CHs-MOFs. However, encapsulation is limited to a few CHs. The synthesis can also be challenging due to potential side reactions between CHs and the other reagents. Additionally, the stability and reproducibility can be problematic, with weak interactions potentially leading to desorption of CHs-MOFs over time.

- CHs-MOFs prepared using CHs as building blocks. This strategy is practically limited to cyclodextrin-MOFs, which are also water-soluble and thus have limited applicability for biomedical applications unless appropriately modified. The use of other types of carbohydrates to obtain crystalline MOFs remains an open challenge.

As a result, ongoing research should focus on addressing these challenges alongside new research on CHs-MOFs, potentially leading to a new era in biomedical applications. In this context, the development of CHs-MOFs is greatly enhanced through various advanced synthesis and characterization techniques that optimize the interaction between carbohydrates and MOFs, thereby improving their biomedical applications. Techniques such as layer-by-layer (LbL) assembly provides precise control over MOF coatings for applications in biosensing or drug release, and green synthesis approaches emphasize environmental sustainability by utilizing renewable materials and non-toxic solvents. Click chemistry enables efficient functionalization of MOFs with carbohydrates, enhancing their biological functionality, while electrochemical synthesis

allows for precise control of reaction conditions to optimize carbohydrate interactions. Additionally, high-throughput screening and computational design techniques accelerate the discovery and development of CHs-MOFs by enabling rapid testing and predictive modelling. Together, these methods offer a comprehensive framework for fine-tuning CHs-MOFs properties, addressing challenges related to stability, scalability, and biocompatibility for applications such as drug delivery and biosensing. The search for smart, innovative solutions to the preparation of novel CHs-MOFs could pave the way for real-world biomedical applications. Despite over 100 000 MOF structures being catalogued in the Cambridge Structural Database (CSD), and the theoretical number of possible MOF structures being nearly limitless, only two MOFs have entered human trials to date.<sup>135</sup> This limited transition to industrial production, coupled with ongoing debates about its efficiency, leaves room for ground-breaking discoveries, inviting the smartest and most creative researchers to push the boundaries of CHs-MOFs development.

## Data availability

This is a review manuscript and does not contain any primary data. All data discussed and analyzed in this review are derived from previously published studies, which are appropriately cited in the manuscript. Therefore, no new data were generated or analyzed in support of this work. The cited references provide the source of all data presented. If additional information is needed, readers are encouraged to refer to the original publications listed in the reference section.

## Conflicts of interest

There are no conflicts to declare.

## Acknowledgements

Financial support was provided by the Andalusian Ministry of Economy, Science and Innovation in the framework of the Plan Andaluz de Investigación, Desarrollo e Innovación (PAIDI 2020, programme 54<sup>a</sup> “Investigación científica e innovación,” “POST-DOC\_21\_00594”), the Spanish Ministry of Science and Innovation (Ref: PID2020-119949RB-I00), the Andalusian Ministry of Economy, Science and Innovation cofinanced by the European Regional Development Fund (ERDF) from FEDER and the European Social Fund (ESF) (PY20\_00882 and CV20-04221). The COST action CA-18132 “Functional Glyconanomaterials for the Development of Diagnostic and Targeted Therapeutic Probe” and the COST action CA-22147 “European metal-organic framework network: combining research and development to promote technological solutions” (EU4MOFs) are also acknowledged.

## References

- 1 P. Valverde, A. Ardá, N. C. Reichardt, J. Jiménez-Barbero and A. Gimeno, *MedChemComm*, 2019, **10**, 1678–1691.





- 44 Z. Sun, T. Li, T. Mei, Y. Liu, K. Wu, W. Le and Y. Hu, *J. Mater. Chem. B*, 2023, **11**, 3273–3294.
- 45 I. Roy and J. F. Stoddart, *Acc. Chem. Res.*, 2021, **54**, 1440–1453.
- 46 H. Cai, Y. L. Huang and D. Li, *Coord. Chem. Rev.*, 2019, **378**, 207–221.
- 47 Y. Si, H. Luo, P. Zhang, C. Zhang, J. Li, P. Jiang, W. Yuan and R. Cha, *Carbohydr. Polym.*, 2024, **323**, 121424.
- 48 “Saccharose” etymology: from Latin ‘saccharum,’ in turn from Greek ‘σακχαρον’ (sakkharon), from Arabic ‘(as)sokkar,’ from Persian ‘shakar,’ from Pali ‘sakkharā,’ from Sanskrit ‘शर्करा’ (śarkarā), meaning “sand, gravel, sugar”.
- 49 IUPAC, 1995, 67, 1307. Glossary of class names of organic compounds and reactivity intermediates based on structure, IUPAC Recommendations 1995, on page 1325, DOI: [10.1351/goldbook.C00820](https://doi.org/10.1351/goldbook.C00820).
- 50 S. J. Richards and M. I. Gibson, *JACS Au*, 2021, **1**, 2089–2099.
- 51 K. Kim, S. Lee, E. Jin, L. Palanikumar, J. H. Lee, J. C. Kim, J. S. Nam, B. Jana, T. H. Kwon, S. K. Kwak, W. Choe and J. H. Ryu, *ACS Appl. Mater. Interfaces*, 2019, **11**, 27512–27520.
- 52 H. Hamed, S. Moradi, S. M. Hudson, A. E. Tonelli and M. W. King, *Carbohydr. Polym.*, 2022, **282**, 119100.
- 53 Q. Xu, J. E. Torres, M. Hakim, P. M. Babiak, P. Pal, C. M. Battistoni, M. Nguyen, A. Panitch, L. Solorio and J. C. Liu, *Mater. Sci. Eng., R*, 2021, **146**, 100641.
- 54 T. H. Shin, P. K. Kim, S. Kang, J. Cheong, S. Kim, Y. Lim, W. Shin, J. Y. Jung, J. D. Lah, B. W. Choi and J. Cheon, *Nat. Biomed. Eng.*, 2021, **5**, 252–263.
- 55 K. Yang, J. Liu, L. Luo, M. Li, T. Xu and J. Zan, *RSC Adv.*, 2023, **13**, 7250–7256.
- 56 Y. Toomari, H. Ebrahimpour, M. Pooresmaeil and H. Namazi, *Polym. Bull.*, 2022, **80**, 4407–4428.
- 57 M. B. Mukherjee, R. Mullick, B. U. Reddy, S. Das and A. M. Raichur, *ACS Appl. Bio Mater.*, 2020, **3**, 7598–7610.
- 58 J. D. Xiao, R. Li and H. L. Jiang, *Small Methods*, 2023, **7**, 2300702.
- 59 A. Zuliani, N. Khair and C. Carrillo-Carrión, *Anal. Bioanal. Chem.*, 2023, **415**, 2005–2023.
- 60 S. F. A. Rizvi, H. Zhang and Q. Fang, *Med. Res. Rev.*, 2024, **44**, 2420–2471.
- 61 A. Zhang, K. Meng, Y. Liu, Y. Pan, W. Qu, D. Chen and S. Xie, *Adv. Colloid Interface Sci.*, 2020, **284**, 102261.
- 62 L. Guerrini, R. A. Alvarez-Puebla and N. Pazos-Perez, *Materials*, 2018, **11**, 1154.
- 63 L. Wang, Z. Li, Y. Wang, M. Gao, T. He, Y. Zhan and Z. Li, *Nanoscale*, 2023, **15**, 10529–10557.
- 64 L. Meng, J. Ren, Z. Liu and Y. Zhao, *J. Drug Delivery Sci. Technol.*, 2022, **70**, 103193.
- 65 Z. Cai, F. Xin, Z. Wei, M. Wu, X. Lin, X. Du, G. Chen, D. Zhang, Z. Zhang, X. Liu and C. Yao, *Adv. Healthcare Mater.*, 2019, **9**, 1900996.
- 66 W. Cai, H. Gao, C. Chu, X. Wang, J. Wang, P. Zhang, G. Lin, W. Li, G. Liu and X. Chen, *ACS Appl. Mater. Interfaces*, 2017, **9**, 2040–2051.
- 67 X. Fu, Z. Yang, T. Deng, J. Chen, Y. Wen, X. Fu, L. Zhou, C. Yu and Z. Zhu, *J. Mater. Chem. B*, 2020, **8**, 1481–1488.
- 68 N. Song, B. Li, D. Li and Y. Yan, *APL Mater.*, 2023, **11**, 081112.
- 69 X. Xu, Y. Chen, Y. Zhang, Y. Yao and P. Ji, *J. Mater. Chem. B*, 2020, **8**, 9129–9138.
- 70 F. Shu, D. Lv, X. L. Song, B. Huang, C. Wang, Y. Yu and S. C. Zhao, *RSC Adv.*, 2018, **8**, 6581–6589.
- 71 V. V. Vinogradov, A. S. Drozdov, L. R. Mingabudinova, E. M. Shabanova, N. O. Kolchina, E. I. Anastasova, A. A. Markova, A. A. Shtil, V. A. Milichko, G. L. Starova, R. L. M. Precker, A. V. Vinogradov, E. Hey-Hawkins and E. A. Pidko, *J. Mater. Chem. B*, 2018, **6**, 2450–2459.
- 72 H. Zhang, Y. Shang, Y. H. Li, S. K. Sun and X. B. Yin, *ACS Appl. Mater. Interfaces*, 2018, **11**, 1886–1895.
- 73 V. R. Cherkasov, E. N. Mochalova, A. V. Babenyshev, J. M. Rozenberg, I. L. Sokolov and M. P. Nikitin, *Acta Biomater.*, 2020, **103**, 223–236.
- 74 S. Javanbakht, M. Pooresmaeil, H. Hashemi and H. Namazi, *Int. J. Biol. Macromol.*, 2018, **119**, 588–596.
- 75 M. Parsaei and K. Akhbari, *Inorg. Chem.*, 2022, **61**, 19354–19368.
- 76 N. Jin, B. Wang, X. Liu, C. Yin, X. Li, Z. Wang, X. Chen, Y. Liu, W. Bu and H. Sun, *J. Nanobiotechnol.*, 2023, **21**, 426.
- 77 W. Chen, M. Yang, H. Wang, J. Song, C. Mei, L. Qiu and J. Chen, *Adv. Healthcare Mater.*, 2024, **13**, 2304000.
- 78 S. Das, P. Kudale, P. Dandekar and P. V. Devarajan, in *Targeted Intracellular Drug Delivery by Receptor Mediated Endocytosis*, ed. P. V. Devarajan, P. Dandekar and A. A. D'Souza, Springer International Publishing, Berlin, 2019.
- 79 A. U. Ortiz, A. P. Freitas, A. Boutin, A. H. Fuchs and F. X. Coudert, *Phys. Chem. Chem. Phys.*, 2014, **16**, 9940–9949.
- 80 R. E. Giménez, E. Piccinini, O. Azzaroni and M. Rafti, *ACS Omega*, 2019, **4**, 842–848.
- 81 M. Moradi, M. Aliomrani, S. Tangestaninejad, J. Varshosaz, H. Kazemian, F. S. Emami and M. Rostami, *Appl. Organomet. Chem.*, 2022, **36**, e6755.
- 82 A. Abednejad, A. Ghaee, J. Nourmohammadi and A. A. Mehrizi, *Carbohydr. Polym.*, 2019, **222**, 115033.
- 83 E. Bellido, T. Hidalgo, M. V. Lozano, M. Guillevic, R. Simón-Vázquez, M. J. Santander-Ortega, Á. González-Fernández, C. Serre, M. J. Alonso and P. Horcajada, *Adv. Healthcare Mater.*, 2015, **4**, 1246–1257.
- 84 D. Bhatt, S. Singh, N. Singhal, N. Bhardwaj and A. Deep, *Anal. Bioanal. Chem.*, 2023, **415**, 659–667.
- 85 W. Ma, B. Yang, J. Li, M. Liu, X. Li and H. Liu, *Microchim. Acta*, 2022, **189**, 253.
- 86 J. Cui, C. Zhang, H. Liu, L. Yang, X. Liu, J. Zhang, Y. Zhou, J. Zhang and X. Yan, *ACS Appl. Mater. Interfaces*, 2023, **15**, 11520–11535.
- 87 J. Hu, W. Wu, Y. Qin, C. Liu, P. Wei, J. Hu, P. H. Seeberger and J. Yin, *Adv. Funct. Mater.*, 2020, **30**, 1910084.
- 88 W. Cao, S. Xie, Y. Liu, P. Ran, Z. Zhang, Q. Fang and X. Li, *Adv. Funct. Mater.*, 2024, **34**, 2312866.



- 89 A. N. Nikam, A. Pandey, S. H. Nannuri, G. Fernandes, S. Kulkarni, B. S. Padya, S. Birangal, G. G. Shenoy, S. D. George and S. Mutalik, *Crystals*, 2022, **12**, 1484.
- 90 Y. Shao, H. Suo, S. Wang, Y. Peng, X. Chu, Z. Long, K. Du, L. Su, X. Sun, X. Wang, Q. Wang, R. Li and B. Wang, *Chem. Eng. J.*, 2024, **481**, 148576.
- 91 X. Hu, R. Li, J. Liu, K. Fang, C. Dong and S. Shi, *Adv. Healthcare Mater.*, 2024, **13**, 2302333.
- 92 Q. Zhou, D. Xie, K. Wang, F. Wang, Q. Wang, Y. Huang, M. Yu, J. Huang and Y. Zhao, *Drug Delivery Transl. Res.*, 2024, DOI: [10.1007/s13346-024-01652-4](https://doi.org/10.1007/s13346-024-01652-4).
- 93 S. Kulkarni, A. Pandey, S. Soman, S. H. Nannuri, A. Kumar, D. Bhavsar, S. D. George, S. Subramanian and S. Mutalik, *Int. J. Biol. Macromol.*, 2024, **278**, 134381.
- 94 Z. Li, S. He, L. Xie, G. Zeng, J. Huang, H. Wang, H. Chen, T. Deng, Y. Xia, C. Huang and Z. Chen, *Adv. Funct. Mater.*, 2024, 2411247, DOI: [10.1002/adfm.202411247](https://doi.org/10.1002/adfm.202411247).
- 95 X. Lu, X. Yu, B. Li, X. Sun, L. Cheng, Y. Kai, H. Zhou, Y. Tian and D. Li, *Adv. Sci.*, 2024, 2405643, DOI: [10.1002/adv.202405643](https://doi.org/10.1002/adv.202405643).
- 96 H. Li, C. Zhang, Y. Chen, Y. Xu, W. Yao and W. Fan, *ACS Nano*, 2024, **18**, 23711–23726.
- 97 Y. Lou, Z. Wang and Y. Wang, *Colloids Surf., A*, 2024, **703**, 135217.
- 98 Q. An, Z. Dai, J. Zhang, H. Hu, J. Wang, X. Cao, Z. Hu, Y. Sun, L. Tian and X. Zheng, *ACS Appl. Nano Mater.*, 2024, **7**, 11757–11766.
- 99 X. Wan, Y. Zhang, T. Zheng, W. Pan, W. Zhu, N. Li and B. Tang, *Mater. Today Nano*, 2024, **26**, 100484.
- 100 X. Sun, H. Li, L. Qi, F. Wang, Y. Hou, J. Li and S. Guan, *Prog. Org. Coat.*, 2024, **187**, 108177.
- 101 A. R. Ahangarkolaee, A. Binaeian, A. H. Kasgari, P. Valipour and E. Binaeian, *J. Porous Mater.*, 2024, **31**, 2193–2203.
- 102 Q. Sun, T. Yuan, G. Yang, D. Guo, L. Sha and R. Yang, *Int. J. Biol. Macromol.*, 2023, **253**, 127519.
- 103 C. R. Quijia, A. Ocaña, C. Alonso-Moreno, R. C. Galvão Frem and M. Chorilli, *J. Mol. Struct.*, 2024, **1305**, 137801.
- 104 A. Taghikhani, M. Babazadeh, S. Davaran and E. Ghasemi, *Colloids Surf., B*, 2024, **243**, 114122.
- 105 M. Dousti, A. Golmohamadpour, Z. Hami and Z. Jamalpoor, *Nanotechnology*, 2024, **35**, 145101.
- 106 S. Zhang, H. Liu, D. Fu, H. Zhao, D. Zhang and T. Lü, *J. Chromatogr. A*, 2024, **1735**, 465347.
- 107 X. Mao, Y. Lu, X. Zhang and Y. Huang, *Talanta*, 2018, **188**, 161–167.
- 108 M. Pooresmaeil and H. Namazi, *Int. J. Pharm.*, 2022, **625**, 122112.
- 109 A. Guo, M. Durymanov, A. Permyakova, S. Sene, C. Serre and J. Reineke, *Pharm. Res.*, 2019, **36**, 53.
- 110 B. Gao, K. Yang, M. Yang, W. Li, T. Jiang, R. Gao, Y. Pei, Z. Pei and Y. Lv, *Chem. Commun.*, 2024, **60**, 8892–8895.
- 111 P. H. Tong, L. Zhu, Y. Zang, J. Li, X. P. He and T. D. James, *Chem. Commun.*, 2021, **57**, 12098–12110.
- 112 M. D. J. Velásquez-Hernández, E. Astria, S. Winkler, W. Liang, H. Wiltsche, A. Poddar, R. Shukla, G. Prestwich, J. Paderi, P. Salcedo-Abraira, H. Amenitsch, P. Horcajada, C. J. Doonan and P. Falcaro, *Chem. Sci.*, 2020, **11**, 10835–10843.
- 113 E. Astria, M. Thonhofer, R. Ricco, W. Liang, A. Chemelli, A. Tarzia, K. Alt, C. E. Hagemeyer, J. Rattenberger, H. Schroettner, T. Wrodnigg, H. Amenitsch, D. M. Huang, C. J. Doonan and P. Falcaro, *Mater. Horiz.*, 2019, **6**, 969–977.
- 114 N. Hammi, S. El Hankari, N. Katir, N. Marcotte, K. Draoui, S. Royer and A. El Kadib, *Microporous Mesoporous Mater.*, 2020, **306**, 110429.
- 115 P. Raju, K. Balakrishnan, M. Mishra, T. Ramasamy and S. Natarajan, *J. Drug Delivery Sci. Technol.*, 2022, **70**, 103223.
- 116 R. Zhao, T. Chen, Y. Li, L. Chen, Y. Xu, X. Chi, S. Yu, W. Wang, D. Liu, B. Zhu and J. Hu, *Food Chem.*, 2024, **448**, 139167.
- 117 Y. Liu, C. Yuan, B. Cui, M. Zhao, B. Yu, L. Guo, P. Liu and Y. Fang, *Food Chem.*, 2024, **443**, 138543.
- 118 A. Cioci, P. Benzi, C. Canepa, L. Mortati, A. de la Paz, I. M. Garnica-Palafox, F. M. Sánchez-Arévalo, R. C. Dante and D. Marabello, *Inorganics*, 2024, **12**, 231.
- 119 R. Zhao, T. Chen, Y. Li, L. Chen, Y. Xu, X. Chi, S. Yu, W. Wang, D. Liu, B. Zhu and J. Hu, *Food Chem.*, 2024, **448**, 139167; D. Marabello, P. Antoniotti, P. Benzi, C. Canepa, E. Diana, L. Operti, L. Mortati and M. P. Sassi, *J. Mater. Sci.*, 2015, **50**, 4330–4341.
- 120 Y. Liu, C. Yuan, B. Cui, M. Zhao, B. Yu, L. Guo, P. Liu and Y. Fang, *Food Chem.*, 2024, **443**, 138543; D. Marabello, P. Antoniotti, P. Benzi, C. Canepa, L. Mortati and M. P. Sassi, *Acta Crystallogr., Sect. B: Struct. Sci., Cryst. Eng. Mater.*, 2017, **73**, 737–743.
- 121 B. P. Carpenter, A. R. Talosig, B. Rose, G. Di Palma and J. P. Patterson, *Chem. Soc. Rev.*, 2023, **52**, 6918–6937.
- 122 Y. Xu, Y. Liu, H. Han and Z. Ma, *Chem. Mater.*, 2022, **34**, 4242–4247.
- 123 Z. Meng, B. Yu, Y. Chen, Y. Deng, H. Li, J. Yao and H. Y. Yang, *Chem. Eng. Sci.*, 2024, **284**, 119527.
- 124 T. De Villenoisy, N. Ho, S. Chen, X. Zheng, C. C. Sorrell, Y. Zhang and P. Koshy, *Mater. Chem. Phys.*, 2023, **309**, 128448.
- 125 C. M. Cova, L. Boffa, M. Pistocchi, S. Giorgini, R. Luque and G. Cravotto, *Molecules*, 2019, **24**, 2681.
- 126 A. Zuliani, M. Cano, F. Calsolaro, A. R. Puente Santiago, J. J. Giner-Casares, E. Rodríguez-Castellón, G. Berlier, G. Cravotto, K. Martina and R. Luque, *Sustainable Energy Fuels*, 2021, **5**, 720–731.
- 127 A. Zuliani, S. Chen and R. Giorgi, *Appl. Mater. Today*, 2023, **30**, 101716.
- 128 A. Zuliani, D. Bandelli, D. Chelazzi, R. Giorgi and P. Baglioni, *J. Colloid Interface Sci.*, 2022, **614**, 451–459.
- 129 C. M. Cova, A. Zuliani, R. Manno, V. Sebastian and R. Luque, *Green Chem.*, 2020, **22**, 1414–1423.
- 130 M. Chang, C. Tang, C. C. Wang and C. Zhao, *Prog. Nat. Sci.: Mater. Int.*, 2024, **34**, 66–73.
- 131 H. Ding, Q. Xia, J. Shen, C. Zhu, Y. Zhang and N. Feng, *Colloids. Surf. B Biointerfaces*, 2023, **232**, 113607.



- 132 C. M. Cova, V. Ramos, A. Escudero, J. P. Holgado, N. Khiar and A. Zuliani, *Green Chem.*, 2024, DOI: [10.1039/D4GC03743J](https://doi.org/10.1039/D4GC03743J).
- 133 A. Bandyopadhyay, T. Das, S. Nandy, S. Sahib, S. Preetam, A. V. Gopalakrishnan and A. Dey, *Naunyn-Schmiedeberg Arch.*, 2023, **396**, 3417–3441.
- 134 M. A. Rahim, N. Jan, S. Khan, H. Shah, A. Madni, A. Khan, A. Jabar, S. Khan, A. Elhissi, Z. Hussain, H. C. Aziz, M. Sohail, M. Khan and H. E. Thu, *Cancers*, 2021, **13**, 6710.
- 135 R. S. Forgan, *Commun. Mater.*, 2024, **5**, 46.

